APPLICATION OF NEW CHEMICAL TEST REACTIONS TO STUDY MASS TRANSFER FROM SHRINKING DROPLETS AND MICROMIXING IN THE ROTOR-STATOR MIXER

Jerzy Bałdyga, Michał Kotowicz[*]

Warsaw University of Technology, Faculty of Chemical and Process Engineering, ul. Waryńskiego 1, Warsaw, Poland

A pair of fast competitive reactions, neutralization and 2,2-dimetoxypropane (DMP) hydrolysis, has been applied do study mass transfer and micromixing in a T 50 Ultra-Turrax® - IKA rotor-stator device. In experiments the dispersed organic phase containing p-Toluenesulfonic acid (pTsOH) dissolved in diisopropyl ether, whereas the continuous phase was represented by the aqueous solution of sodium hydroxide, 2,2-dimetoxypropane (DMP) and ethanol. During mixing a fast mass transfer of a solute (pTsOH) from organic phase droplets, which were shrinking due to fast dissolution of the organic solvent, was followed by micromixing and chemical reactions in the continuous phase. Measured hydrolysis yields were applied to express effects of mixing on the course of chemical reactions. Modeling was based on application of models describing drop breakup, mass transfer in the liquid-liquid system and micromixing. Combined effects of mass transfer and drop breakage on drop population were expressed using the population balance equations. The model has been used to interpret experimental results, in particular to identify the efficiency of mixing.

Keywords: efficiency of mixing, mass transfer, micromixing, rotor-stator mixer, test reactions

1. INTRODUCTION

Many chemical reactions leading to desirable intermediate and end-products (such as pharmaceutical intermediates and other fine chemicals) are accompanied by side reactions producing undesired byproducts. The creation of byproducts decreases the yield of desired reactions and requires costly product separation. Even when the desired reaction is very fast compared to undesired ones, its rate can be controlled by mass transfer and micro-mixing, and the final yield and selectivity can result then from competition between the desired, mass transfer and micro-mixing controlled chemical reaction and other, slower reactions. Hence, to control product distribution of complex chemical reactions one needs not only to have detailed information on their kinetics and thermodynamics but also understand and interpret the effects of flow, mass transfer and following it micro-mixing on their course.
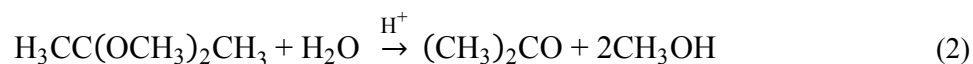
Test chemical reactions are commonly used as molecular probes to investigate mixing processes in both homogeneous and heterogeneous liquid-liquid systems. To employ the set of chemical reactions as test reactions one needs to know reaction schemes, reaction kinetics (at least one reaction must be faster than the mixing rate) and analytic methods to determine product distribution. Reagents and products should be stable and not toxic. Many different systems were proposed either to study micromixing in single-phase systems (Bałdyga and Bourne, 1990; Bałdyga and Bourne, 1999; Bałdyga et al., 1998; Fournier et al., 1996) or to study mass transfer in two-phase liquid-liquid systems (Jasińska et al.,

*Corresponding authors, e-mail: m.kotowicz@ichip.pw.edu.pl

2013b; Jasińska et al., 2016). By choosing a proper one and treating product distribution as the segregation index, one can compare mixing intensity in different systems. One can identify as well the time constant for mixing and mass transfer. Moreover, it is possible to relate the product distribution to such a parameter as the rate of energy dissipation, and obtain as well relations necessary to identify the minimum rate of energy dissipation required for measured product distribution and related mixing efficiency. It has been shown (Jasińska et al., 2013a) that mixing efficiency of rotor-stator mixers for homogeneous systems decreases with increasing rotational speed due to shrinking of reaction zone to the feed inlet and increasing effects of inertial-convective mixing. One can as well compare energetic efficiencies of mass transfer in rotor-stator mixers differing in geometry (Jasińska et al., 2013b). Having experimental data one can validate the phenomenological micromixing and mass transfer models including modeling employing CFD. Validated models can be used to optimize system geometry and process parameters (such as feeding rate and power input). Modeling can be used to increase desired product yield and decrease operational costs. Comprehensive reviews on the application of chemical test reactions to study micromixing and mass transfer in single-phase and two-phase systems can be found in the papers by (Bourne, 2003) and (Jasińska, 2015). In the case of two-phase test systems, different reacting species were dissolved both in the continuous phase and a solvent forming the dispersed phase. The solvent was not soluble in the continuous phase, so the volume fraction of the dispersed phase was constant during the process. However, there are industrial applications where the dispersed phase shrinks during the process. In next section of this paper a new system of test reactions for mixing in liquid-liquid systems is proposed. Contrary to other studies on two-phase systems, the proposed system features fast dissolution of the dispersed phase in the reaction environment.

2. MATERIALS AND METHODS

In this work we consider the case of fast mass transfer of solute from droplets that are shrinking due to fast dissolution of the organic phase, dispersed in the continuous aqueous phase. The dispersed organic phase consisted of a solvent (mixture of diisopropyl ether and ethanol) and *p*-toluenesulfonic acid (pTsOH) being an acidic reactant in the system of test reactions. The continuous phase was represented by the aqueous solution of sodium hydroxide (alkaline reactant), 2,2-dimetoxypropane (DMP) and ethanol.

$$NaOH + pTsOH \rightarrow H_2O + pTsONa \tag{1}$$

$$H_3CC(OCH_3)_2CH_3 + H_2O \xrightarrow{H^+} (CH_3)_2CO + 2CH_3OH \tag{2}$$

The first reaction can be treated as instantaneous, the second reaction is catalyzed by hydrogen ions H^+ and can be treated as fast. Equations (1) and (2) represent modification of the set of test reactions proposed earlier (Bałdyga et al., 1998) for homogeneous systems. In the present case ethanol was used to increase solubility of pTsOH in the ether and its volume fraction in the organic phase was equal to 0.25. The continuous, aqueous phase contained 2,2-dimethoxypropane (DMP), NaOH and ethanol. Ethanol was used as well as an internal standard for chromatographic analysis (GC). The volume fraction of organic phase was 0.014 and the molar ratios of base, acid and DMP were respectively 1.05:1.0:1.05. The excess of base was required to maintain stability of DMP before determining the concentrations after performing reactions. In Table 1, initial concentrations of applied species are presented.

Experiments were carried out in the semibatch manner in a T 50 Ultra-Turrax® - IKA rotor-stator mixer placed in a rig shown in Figure 1. The rig was placed under fume hood. The diameters of the stator and the rotor were equal to 45 mm and 36 mm respectively; the gap size was equal to 0.5 mm. The rotor-stator mixers are characterized by high energetic efficiency of dispersion processes due to

focused delivery of energy to the active high-shear regions that occupy a very small fraction of internal mixer space (Jasińska et al., 2013b; Jasińska et al., 2016). Due to pumping capabilities of the rotor-stator mixer, no additional pump was required in the experimental setup. The initial temperature for each experiment was 25°C and the increase of temperature during 2 minute experiment was less than 5 degrees for maximum rotational velocity. The inlet of organic phase was situated before the main inlet to the rotor stator vessel. After an addition of organic phase, the mixer was working for 20 seconds at a chosen rotational speed and during that time the inlet of organic phase was flushed with the reaction mixture. Then samples for chromatographic analysis were collected at the slowest rotational speed to prevent further heating of the mixture. Three or four samples were collected at 10 second intervals to check the mixture uniformity and put into cool (5°C) store. Uniformity was achieved for all samples; the difference in ether concentration in different samples was lower than 5% and increased with the time after which the given sample was collected. Samples were analysed on a HP 6890 gas chromatograph with a 30m column model RTX 1701. The chromatograph was set with the initial oven temperature of 40°C, whereas the speed of temperature growth was 7°C/min and time of analysis was equal to 10.5 min. Injection volume was 0.5 μL and samples during collection were diluted 10 times so the salt concentration was less than 0.4 mmol/dm^3. The generation of methanol was quantified and experiments were considered as valid only when proper molar balances for DMP and its products were obtained. In Table 2 below, results for cases 1 and 2 (Table 1) are shown.

Table 1. Composition of reaction mixtures and initial concentrations. Two variants of composition were investigated, Case 1 and Case 2

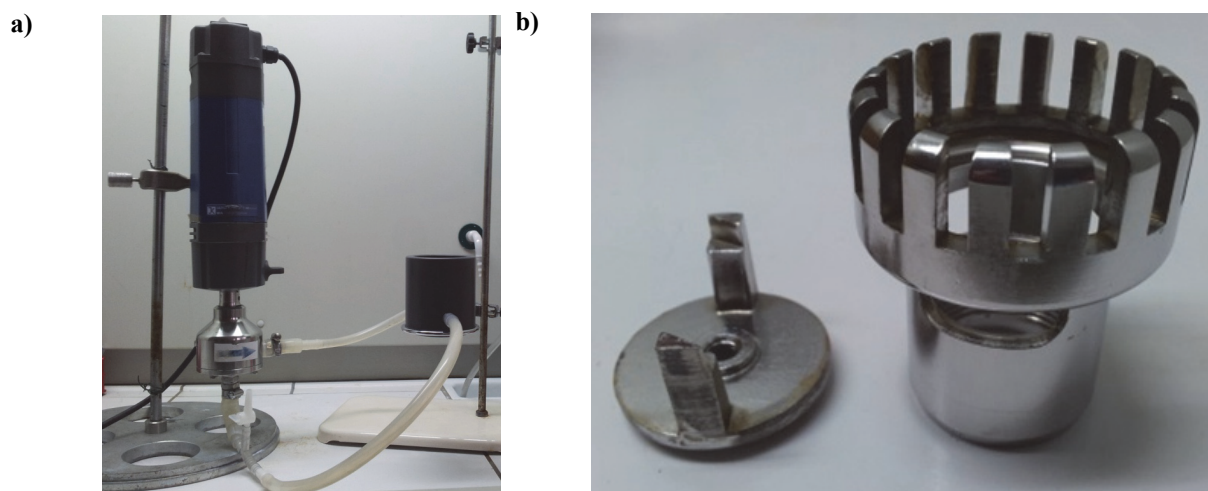| Phase	Substance	Case 1 c_1, mol/m^3	Case 2 c_2, mol/m^3
continuous	ethanol	39.5	39.5
	NaOH	4	3.5
	DMP	4	3.5
dispersed	pTsOH	268	234
	ethanol	4120	4120

Fig. 1. Experimental setup: (a) experimental rig, (b) rotor and stator

Table 2. Conversion of DMP as a function of rotational speed. The first index denotes the case variant (1 or 2), the second shows values before and after the reaction. For the first case, the estimated error for the value of pH before and after reaction is 0.07 and 0.45, for second corresponding values are 0.11 and 0.25. The value of Δn_{err} is deviation from theoretical ratio of change of moles of methanol to DMP, which equals 2

N [1/min]	Q [ml/s]	t_{in} [s]	$\varepsilon_{N,Q}$ [m²/s³]	pH$_{1,0}$	pH$_{1,1}$	$\Delta n_{DMP,1}$ [%]	Δn_{err} [%]	pH$_{2,0}$	pH$_{2,1}$	$\Delta n_{DMP,2}$ [%]	Δn_{err} [%]
4000	41	4.4	579	10.97	8.68	-41.9	-7.5	10.98	8.33	-42.44	-2.0
5200	65	3.4	1417	10.97	8.86	-41.02	-1.3	10.99	8.47	-41.68	-1.5
6400	94	2.6	2907	10.95	8.52	-40.83	-2.0	11.0	8.43	-40.26	-3.0
7600	108	2.1	4772	10.98	8.75	-36.63	-4.5	11.0	8.28	-35.38	+4.0
8800	119	1.9	7191	11.02	8.73	-34.48	-0.5	10.9	8.47	-33.58	-0.5
10000	132	1.7	10404	11.0	8.37	-29.15	-5.0	10.93	8.49	-20.53	+2.0

The feeding time of organic phase t_{in} was roughly proportional to volumetric flow rate of the main stream Q and is shown in Table 2 below. The rate of energy dissipation was calculated according to Eq. (3). This equation is based on the two-term expression for the power number as suggested by (Bałdyga et al. 2007). It includes the effects of the rotor speed and the pumping rate, with constants P_{oz} and K equal to 0.147 and 14.49, respectively (Cheng et al., 2013). The constants are characteristic to dual ultrafine teethed rotor stator mixers.

$$\varepsilon_{N,Q} = \frac{P}{\dot{M}\tau} = \frac{1}{\tau}\left(\frac{P_{oz}N^3D^5}{Q} + KN^2D^2\right) \qquad (3)$$

To model the interphase mass transfer from shrinking droplet, two interface concentrations are assumed to be in equilibrium. It is further assumed that the composition of the acid dissolved in the organic phase is constant, at least in large droplets, due to fast droplets shrinking that is faster than molecular diffusion. It is also assumed that the partition coefficient for the system aqueous solution - diisopropyl ether does not depend on concentration, so there exists linear equilibrium relationship between compositions of the solvent within the droplet and at interface, which is represented by constant κ, $\kappa = c'_i/\rho_{org}$. The rate of dissolution of a spherical droplet of diameter d is thus given by (Eq. 4):

$$\frac{d(V_d\rho_{org})}{dt} = -k_L(c'_{si} - c')\pi d^2 \cong -k_L\kappa\rho_{org}\pi d^2 \qquad (4)$$

To determine the value of the partition coefficient, solutions of diisopropyl ether, pTsOH and ethanol were prepared with varying concentrations of acid (216 - 267 mol/m³) and volume fraction of ethanol equal to 0.25. Then portions of the organic phase were added drop by drop with a burette to the aqueous solution. The visible two phase system was homogenized with shaking of the flask. The measurement was terminated when no more organic phase could be dissolved in the aqueous phase. Considering that water solubility in ether is negligible, the volume fraction of the organic phase in water was calculated and the constant κ was determined. No significant effect of the concentration of acid in the organic phase on the equilibrium constant was observed and the obtained value of κ was equal to 0.017 ± 0.001. Experiments were performed in the temperature of 25 °C, both for distilled water and solution of reactants as in the test reaction system. No influence of the composition of continuous phase on the partition coefficient was observed.

2. PROPOSED MODEL

To interpret experimental data, a method combining the model of mass transfer with the micromixing engulfment model is proposed. Firstly, Lagrangian model which governs evolution of single droplet is derived. The dispersed phase is denoted by index d and the continuous phase by index c. $D_{s,c}$ denotes the coefficient of molecular diffusion of the solvent in the continuous phase. Assuming constant density of droplets, the rate of change of its volume is given by Eq. (4). The mass transfer coefficient was calculated according to the model proposed by (Polyanin, 1984):

$$k_L = \frac{D_{s,c}}{d_p} 0.620 \left(\frac{\mu_d}{\mu_c} + 1 \right)^{-0.5} Pe_M^{0.5} \tag{5}$$

where $Pe_M = \dfrac{d_p^2}{D_{s,c}} \left(\dfrac{\varepsilon}{\nu} \right)^{0.5}$

Each portion of a droplet containing pTsOH (A) that dissolves in the continuous phase starts to engulf NaOH (B) and DMP (D) rich solution. The growth of A-rich reaction zone for fluid element denoted by i is given by the relation resulting from the self-engulfment model of micromixing (Bałdyga and Bourne, 1989):

$$x_{A,i} = x_{A,i}^0 \frac{e^{Et}}{1 - x_{A,i}^0 \left(1 - e^{Et} \right)} \tag{6}$$

$$x_{A,i}^0 = \frac{\displaystyle\int_{t_i-1}^{t_i} \frac{dV_d}{dt} dt}{V_B \phi + \displaystyle\int_0^{t_i} \frac{dV_d}{dt} dt} \tag{7}$$

where x_A is the volume fraction of A-rich fluid in the engulfed volume, ϕ is the volume fraction of the organic phase represented by traced droplet at initial state. As the reaction of neutralization is instantaneous, it is controlled by micromixing and the mass balance of acid in the engulfed volume is given by (Eq. 8):

$$\frac{d(V_A c_A)}{dt} = E V_A (1 - x_A) \langle c_A \rangle - V_A E (1 - x_A) \langle c_B \rangle \tag{8}$$

$$\frac{d(V_A c_D)}{dt} = E V_A (1 - x_A) (\langle c_D \rangle - c_D) - V_A k_2 c_D c_A \tag{9}$$

$$\frac{d(V_A c_T)}{dt} = -E V_A (1 - x_A) c_T + V_A k_2 c_D c_A \tag{10}$$

$$\frac{d(V_A c_R)}{dt} = -E V_A (1 - x_A) c_R + V_A E (1 - x_A) \langle c_B \rangle \tag{11}$$

The next three equations (Eqs. 9, 10, 11) represent the balance of DMP, acetone and salt in the engulfed volume. Initial droplet diameter for just dispersed droplets can be calculated from Eq. 12 proposed by (Kolmogorov, 1949):

$$d = \frac{C_x \sigma^{0.6}}{\varepsilon^{0.4} \rho_c^{0.6}} \tag{12}$$

Earlier experiments employing test reactions to study micromixing in rotor stator devices indicated that efficiency of mixing decreases with increasing rotor speed (Jasińska et al., 2013a; Jasińska et al., 2013b) to some asymptotic value. Mixing efficiency was originally defined by (Ottino and Macosko, 1980) to estimate energetic effectiveness of the process of mixing between elongated slabs in laminar flow or in the viscous-convective and viscous-diffusive subranges of turbulence. It characterises the ratio of energy really applied to increase the intermaterial area to the whole energy dissipated during the flow. This definition determines the form of the expression for mixing efficiency. (Jasińska et al., 2013a) extended this definition to account for mixing on the molecular scale. They introduce the ideal, reference process of mixing that was described with the reference model, the engulfment model of micromixing. Prediction of the E-model can be used as a calibration curve, which based on experimentally determined X_S values gives the smallest, "theoretical" values of the rate of energy dissipation necessary to obtain experimental X_S, that can be later compared with the energy really used in experiments. Determination of mixing efficiency enables to correct the mixing ($E = 0.058(\varepsilon/v)^{0.5}$) and mass transfer (Eq. 5) parameters.

The influence of efficiency factors on the predicted reaction yield $X_{s,eff}$: $X_S = (N_{D0} - N_D)/N_{D0}$, is fundamental. If they were neglected then conversion would be strongly underestimated and the model would yield conversion of dimetoxypropane, expressed by the product distribution X_S, of less than 1% in the considered energy dissipation range. The model predictions and the experimental data are presented in Fig. 2.
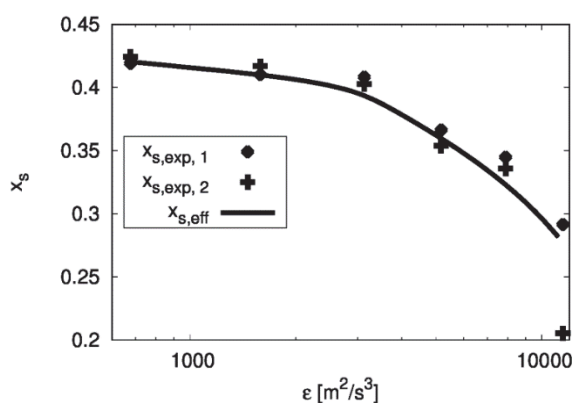

Fig. 2. Predicted $X_{s,eff}$ and observed $X_{s,exp}$ values of the product distribution vs. rate of energy dissipation
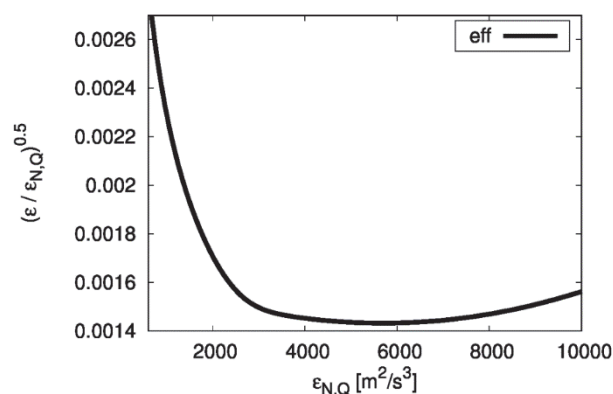
Fig. 3. Mixing efficiency as a function of the rate of energy dissipation

In Fig. 3 the efficiency of mixing is plotted. Figures 2 and 3 show that within the range of energy dissipation between 500–3000 m²/s³, the decomposition yield decreases only slightly, whereas the energetic efficiency of mixing decreases significantly. On the other hand it is interesting that efficiency starts to increase when the rotational speed higher than 6400 rpm is applied. In this range sensitivity of the product distribution to the rotor rotation speed increases. From the viewpoint of energetic efficiency and primary product yield it can be beneficial to carry out a reaction in the rotor stator mixer at full rotor speed.

The Hatta number for the slower reaction, (Eq. 2), is in the range between $0.092 - 0.009$ in the considered range of energy dissipation, which indicates that the reaction is running in the regime of slow reaction from viewpoint of diffusional mass transfer. The Damkőhler number based on the engulfment time constant (Eq. 13), takes values from the range of $0.123 - 12.288$. Characteristic times of micromixing (Eq. 13) (Bałdyga and Bourne, 1999), mass transfer (Eq. 14) and internal mass transfer of acid (Eqs. 15 and 16) indicate that a reaction is controlled by mass transfer of the solvent that determines the rate of drop shrinking. This mechanism persists up to the energy of dissipation of 3000 m²s⁻³, where the orders of magnitude of micromixing and solvent mass transfer time scales

become equal (Fig. 4). Note that $D_{A,d}$ denotes the coefficient of molecular diffusion of pTsOH in the dispersed phase.

$$\tau_E = 12\left(\frac{\nu}{\varepsilon}\right)^{0.5} \tag{13}$$

$$\tau_D = \frac{d}{6k_L} \tag{14}$$

$$\tau_{D,in} = \frac{d}{6k_{L,in}} \tag{15}$$

$$k_{L,in} = \frac{Sh\, D_{A,d}}{d}, \quad Sh = \frac{2}{3}\pi^2 \tag{16}$$
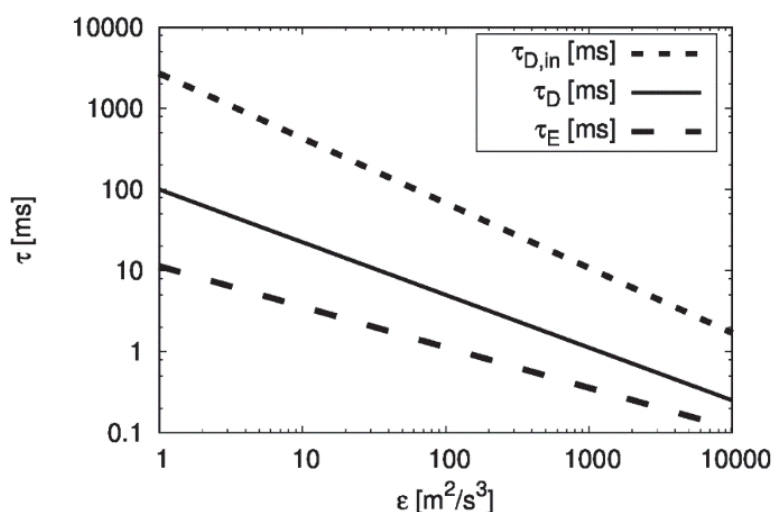

Fig. 4. Time scales for the investigated system as a function of the rate of energy dissipation. The mean residence time for $N = 10000$ rpm is 96 ms and for $N = 4000$ rpm is 310 ms. Time scale for slower reaction is 400 ms

As experiments have shown, the organic phase disappears after the first pass through the mixer. The residence time in the mixing vessel is less than second for all experiments. The model will only predict droplet dissolution correctly if the size of considered droplets will be of the order of micrometers. As shown in the caption of Fig. 5, the multifractal model of drop breakage (Bałdyga and Podgórska, 1998) is applied, as given by Eq. 17, which includes intermittency of turbulence and predicts smaller droplets than Kolmogorov theory of drop breakage (Eq. 12). In fact, Eq. 12 predicts the most probable, not the maximum stable drop size. To calculate the total duration time of the breakage event sequence, a series of droplet breakage events into daughter droplets of equal volume was considered. The initial drop size was assumed to be slightly below the size of the integral length scale for the mixer and the final drop size was defined by the size predicted by multifractal model of turbulence as applied to droplet breakage (Bałdyga and Podgórska, 1998). The equation for maximum stable drop size takes the form:

$$d = C_x^{1.54} L \left(\frac{\sigma}{\rho_c \varepsilon^{2/3} L^{5/3}}\right)^{0.93} \tag{17}$$

The duration of droplet breakage sequence was estimated using the inverse of the breakage frequency for the multifractal model (Eq. 18). Constants required to calculate the upper bound of multifractal exponent and breakage frequency were equal to $C_x = 0.23$, $C_g = 0.0035$. The integral length scale was taken as 0.4 mm based on results of (Jasińska et. al, 2014).

$$\tau_b(d) = \left(C_g \sqrt{ln\left(\frac{L}{d}\right)} \langle \varepsilon \rangle^{1/3} \int_{\alpha_{min}}^{\alpha_x} \frac{d^{\frac{\alpha+2-3f(\alpha)}{3}}}{L} \right)^{-1} \tag{18}$$

The time of droplet breakage $\tau_c = \sum \tau_b$ (Fig. 5), calculated using the multifractal model of turbulence, is small or comparable to time scales of other phenomena depending on final droplet diameter and shows that residence time of few microseconds in high shear stress region suffices to develop high specific surface for the studied liquid-liquid system. The rates of final breakage events leading to the considered drop size, control in fact the overall breakage time (Fig. 5). As breakage takes place in the high shear region of the mixer, following it shrinking of droplets and micromixing are present in the zone of a smaller rate of energy dissipation behind the screen. This explains why efficiency of micromixing is so small as shown in Fig. 3.
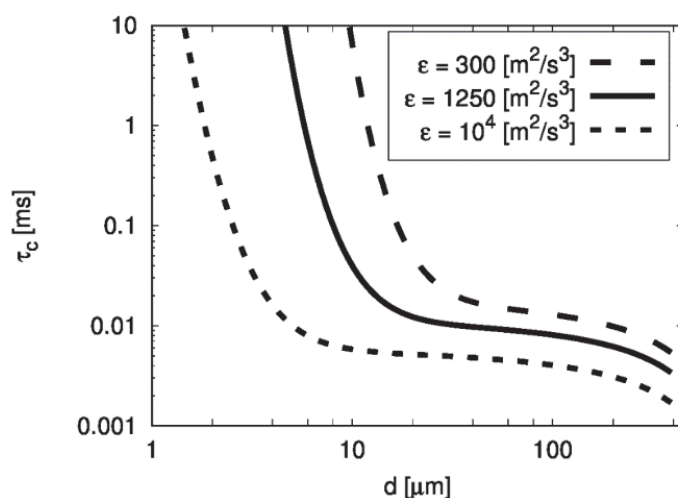

Fig. 5. Time of breakage sequence, $\tau_c = \sum \tau_b$ for a droplet of the initial size equal to 0.39 mm for 3 values of the rate of energy dissipation. Maximum stable droplet sizes d are 8.4, 3.5, 1 μm respectively. This can be compared to droplet size calculated with Kolmogorov theory: 33, 19, 8.2 μm

Having analysed time scales of phenomena identified in the performed experiment, an attempt to simulate evolution of dispersed phase with the population balance model was undertaken. The main reason was to check assumptions on the controlling mechanism for pTsOH transfer to continuous phase at this stage of the process when the droplets are small. Firstly one dimensional model (Eq. 19) including dissolution (Eq. 4) and breakage process kinetics (inverse of Eq. 18) was solved with the direct numerical method. Gauss-Lobatto-Legendre collocation points were used as a type of numerical grid. Advection terms were discretized with differential quadrature rule (Bellman et. al., 1972) derived for 50 GLL points. Integral terms were calculated with Gaussian quadrature rule. Neumann boundary conditions were applied to both ends of the domain (equal to flux at left boundary and zero at right boundary). To cover a broad range of droplet diameters, logarithmic mapping was used for size coordinate. Such nonlinear mapping introduces an error into the numerical method but after analyzing results for the considered cases, the (overestimating) error in conservation of volume of tracked dispersed phase was not higher than 5% of the initial volume. Forward Euler numerical scheme was employed for time discretization and U-shaped parabolic distribution was used as daughter distribution function (Bałdyga and Podgórska, 1998). The evolution of density and moments for various values of the energy dissipation rate can be seen below in Fig. 6. As the solution method calculates density function directly, corresponding moments were calculated from their definitions.

$$\frac{\partial n}{\partial t} + \frac{\partial (nG)}{\partial d_p} = \int_{d_p}^{\infty} g(d') b(d_p / d') n(d') \, d(d') - g(d_p) n(d_p) \tag{19}$$
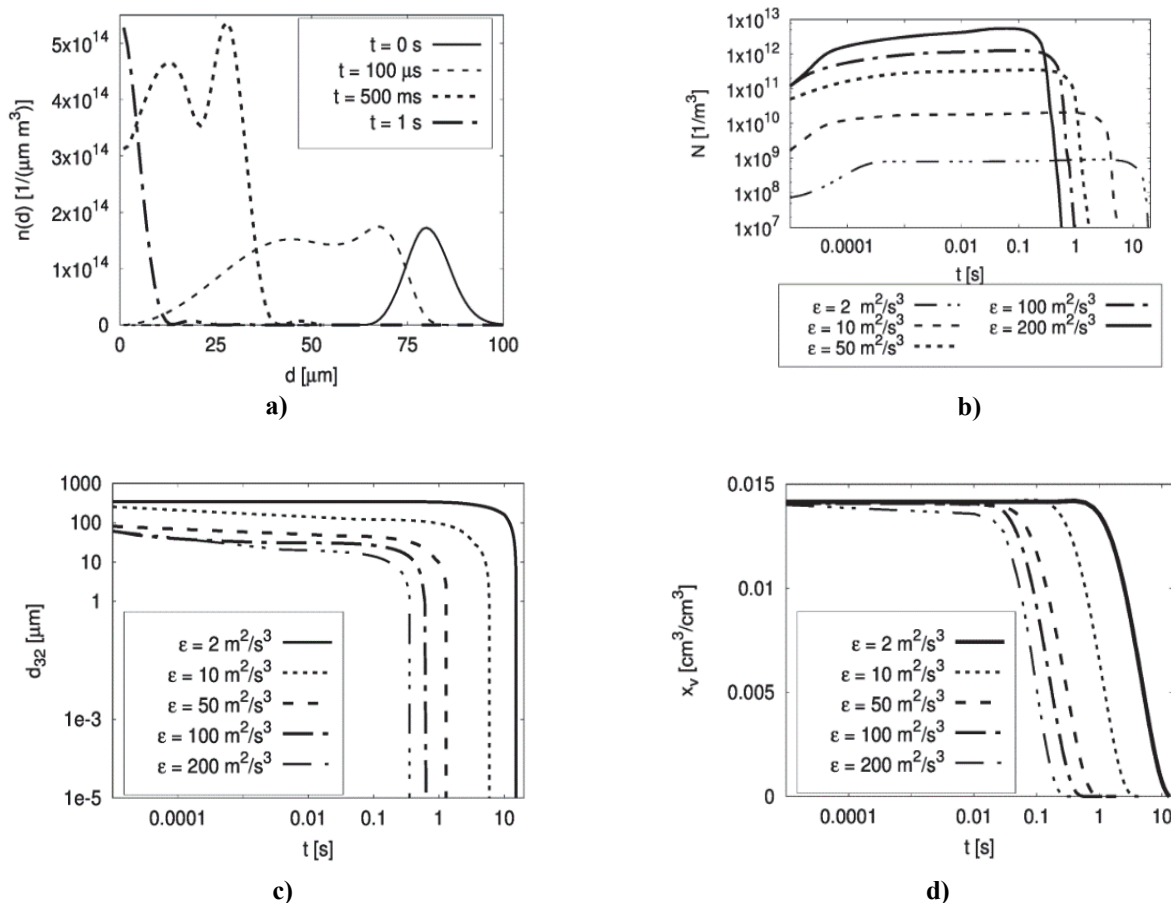
Fig. 6. Prediction of evolution of population of droplets. As initial 1D distribution, the lognormal distribution was assumed with mean 700, 250, 80, 60, 60 μm for subsequent increasing values of rate of energy dissipation and standard deviation equal to 5 μm for each case. (a) number density function $n(d)$ for the rate of energy dissipation of 50 m²/s³, (b) number concentration of droplets N, (c) mean Sauter diameter d_{32} and (d) volume fraction of dispersed phase, x_v

The predictions from simulations are consistent with time scale analysis. During the initial period of the experiment the breakage process dominates, the number of droplets increases rapidly and the amount of dissolved organic phase is negligible. Then drop dissolution process is mostly present and depending on energy dissipation rate it can take from 0.1 to 10 seconds. Figure 6a, where the number density function $n(d)$ is presented, shows that bimodal distribution is formed. This is direct consequence of using the U-shaped daughter distribution function.

To check how the composition of droplets changes during the process, the population balance model was extended by introducing acid concentration as the second state space coordinate. Because the solubility of *p*-toluenesulfonic acid in the organic phase is much lower that in water it can be assumed that except shrinking, only internal mass trasfer will be meaningfull for overall transfer of acid into the aqueous solution. Using the correlation for Sherwood number presented above (Eq. 16) the expression for acid trasfer is given by (Eq. 20):

$$C_R = \frac{dC_A}{dt} = -k_{L,in} c_A \frac{A}{V} = -k_{L,in} c_A \frac{6}{d_p} \tag{20}$$

$$\frac{\partial n}{\partial t} + \frac{\partial (nG)}{\partial d_p} + \frac{\partial (nC_R)}{\partial c_A} = \int_{d_p}^{\infty} g(d') b(d_p / d') n(d', c_A) d(d') - g(d_p) n(d_p, c_A) \tag{21}$$

The two dimensional population balance (Eq. 21), was solved with a similar method as applied for 1D case and following results were obtained (Figs. 7 and 8). For an additional dimension, Neuman boundary conditions were applied in an analogous manner as for 1D problem.
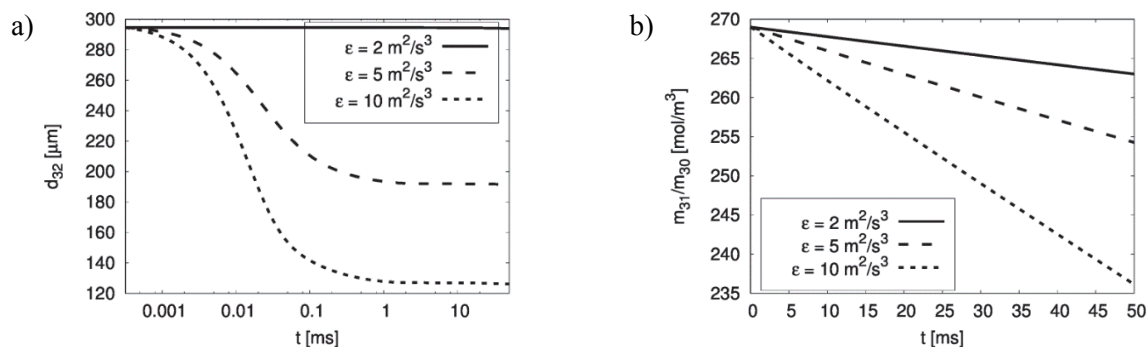

Fig. 7. Results of simulation of 2D population: (a) evolution of the mean Sauter diameter d_{32} and (b) mean concentration of a solute A in population of droplets m_{31}/m_3. Duration of simulation was 50ms

For the energy dissipation rate equal to 2 m²/s³ the starting drop diameter is nearly equal to that predicted by the breakage model and no further breakage is observed (Fig. 7a). For higher values of the rate of energy dissipation the maximum stable drop size is observed after about 100 µs and this time decreases with increasing the rate of energy dissipation. Figure 7b shows some decrease in time of the average solute concentration. Figure 8 explains this effect; it illustrates the evolution in time of the 2D distribution. Clearly, initially there is just a drift of the distribution in the direction of smaller droplets due to breakage without observable effects of pTsOH diffusion. When much smaller droplets are created due to shrinking and breakage, the effects of molecular diffusion become significant. This means that at final stages of droplet life, the assumption that the controlling mechanism for pTsOH transfer to the continuous phase is droplet shrinking, is not fulfilled and both mechanisms of drop shrinking and molecular diffusion are influential.
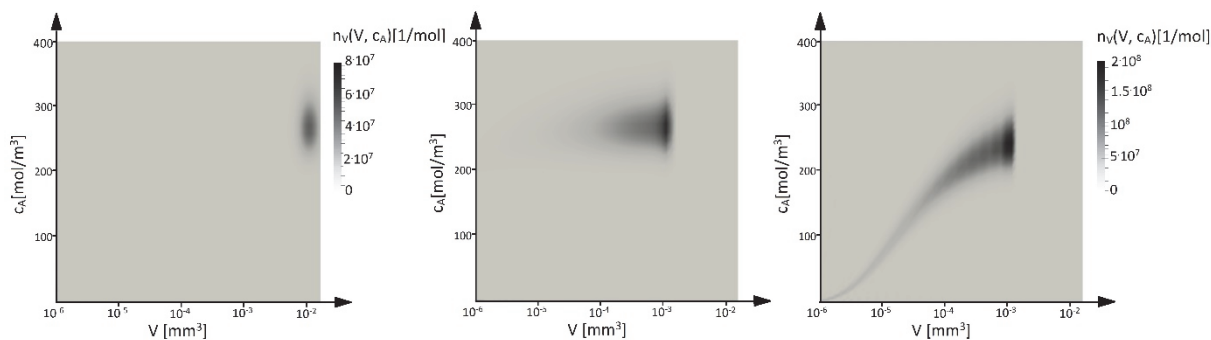

Fig. 8. Evolution of two dimensional volume density function $n_v(V, c_A)$ [1/mol] during simulation for rate of energy dissipation equal to 10 m²/s³. The following pictures present results at the initial moment, after 2ms and 50ms of simulation. Note that the middle and right figures have the same scale. As in 1D case, 2D lognormal distribution with means equal to 300µm, 265 mol/m³ m and standard deviations for size and concentration equal to 5µm, 1 mol/m³ respectively was used to describe population at the initial period of the process

4. CONCLUSIONS

A new set of competitive test reactions to be applied in a liquid-liquid system was proposed. Simplicity of the reaction scheme as well as a simple and direct method of determination of product distribution makes this new set of test reactions a decent tool for investigation of product yields in mixers of any

type and for any mode of operation. It was proved that this system is suitable for investigating mixing processes in rotor stator devices. The conclusions presented by earlier investigators (Jasińska et al., 2013a; Jasińska et al., 2013b), that mixing efficiency in rotor stator devices for both homogeneous and heterogeneous systems decreases with increasing the rotational rotor speed, were confirmed and mixing efficiency factors were obtained based on experimental data. It has been shown that the engulfment model of micromixing, commonly used to describe homogeneous systems, can be combined with the mass transfer model for liquid-liquid systems and applied to model the evolution of mass transfer in a system with droplet shrinking in the continuous phase.

It should be pointed out that the identified values of the efficiency of mixing (mass transfer and micromixing) depend on the applied reference models, i.e. the engulfment model of micromixing, the mass transfer model by (Polyanin, 1984) and the model for the maximum stable drop size by (Kolmogorov, 1949). These models were chosen because they were verified experimentally by many researchers and can be treated as reliable, at least regarding their form. Although the application of other models is possible, one should always inform which model was used.

Finally, 1D and 2D population balance models were used to simulate the evolution of dispersed phase. Results showed that the assumption about constant acid concentration during droplet dissolution can be too coarse approximation for very small droplets and future work should address that issue.

SYMBOLS

b	daughter distribution function
c	concentration, mol/m^3
c'	concentration, kg/m^3
c'_i	interfacial concentration, kg/m^3
$\langle c \rangle$	mean concentration, mol/m^3
C_x	proportionality constant for expression for maximum stable drop size
C_g	proportionality constant for multifractal model
C_R	rate of change of acid concentration, mol/(m$^3 \cdot$ s)
d, d_p	droplet diameter, m
D	rotor diameter, m
$D_{S,C}$	diffusion coefficient of solvent in continuous phase, m^2/s
$D_{A,d}$	diffusion coefficient of pTsOH in dispersed phase, m^2/s
eff	mixing efficiency factor
E	engulfment parameter, 1/s
$f(\alpha)$	multifractal spectrum, according to (Bałdyga and Podgórska, 1998)
g	breakage frequency, 1/s
k_2	kinetic constant of slower reaction, m^3/(mol·s)
k_L	external mass transfer coefficient, m/s
$k_{L,in}$	internal mass transfer coefficient, m/s
K	constant related to flow term in power expression
L	integral length scale of turbulence, m
m	moment calculated from number density function
$\dot{M}$	mass flow rate, kg/s
$n(d)$	1D number density function, 1/(μm·m^3)
$n_v(V,c_A)$	2D volume density function, 1/mol

J. Bałdyga, M. Kotowicz, Chem. Process Eng., 2017, 38 (3), 477-489

PAN
POLSKA AKADEMIA NAUK

N	rotational rotor speed, s^{-1}
P	power input, W
P_{oz}	power number at zero flow rate
t_{in}	feeding time, s
Q	flow rate, m^3/s
V_A	total volume of organic phase, m^3
V_B	total volume of continuous phase, m^3
V_d	droplet volume, m^3
$X_{s,eff}$	predicted reaction yield
$X_{s,exp}$	experimental reaction yield
x_A	volume fraction of A-rich fluid in micromixing model
α	multifractal exponent
ε	energy dissipation rate, m^2/s^3
$\varepsilon_{N,Q}$	overall energy dissipation rate in rotor-stator device, m^2/s^3
κ	solubility constant of diisopropyl ether in water, partition coefficient
μ_c	dynamic viscosity of continuous phase, $kg/(m \cdot s)$
μ_d	dynamic viscosity of dispersed phase, $kg/(m \cdot s)$
ν	kinematic viscosity of continuous phase, m^2/s
ρ_c	density of continuous phase, kg/m^3
ρ_{org}	density of organic phase, kg/m^3
σ	interfacial tension, N/m
τ	mean residence time in rotor stator, s
τ_b	time scale of drop breakage, s
τ_c	time necessary to break a droplet to its final size, ms
τ_E	micromixing time scale, s
τ_D	mass transfer time scale, s
$\tau_{D,in}$	internal mass transfer time scale, s
ϕ	volume fraction of organic phase represented by single droplet

Subscripts

A	pTsOH
B	NaOH
D	DMP
R	salt
s	solvent
T	acetone

REFERENCES

Bałdyga J., Bourne J.R., 1989. Simplification of micromixing calculations. II. New applications. *The Chem. Eng. J.*, 42, 93-101. DOI: 10.1016/0300-9467(89)85003-8.

Bałdyga J., Bourne J.R., 1990. The effect of mixing on parallel reactions. *Chem. Eng. Sci.*, 45, 907-916. DOI: 10.1016/0009-2509(90)85013-4.

Bałdyga J., Bourne J.R., 1999. *Turbulent mixing and chemical reactions*. Willey, Chichester.

Bałdyga J., Bourne J.B., Walker B., 1998. Non-isothermal micromixing in turbulent liquids: Theory and experiment. *Canadian J. Chem. Eng.*, 76, 641-649. DOI: 10.1002/ cjce.5450760336.

Bałdyga J., Kowalski A., Cooke M., Jasińska M., 2007. Investigations of micromixing in a rotor-stator mixer. *Chem. Process Eng.*, 28, 867-877.

Bałdyga J., Podgórska W., 1998. Drop break-up in intermittent turbulence: Maximum stable and transient sizes of drops. *Canadian J. Chem. Eng.*, 76(3), 456-470. DOI: 10.1002/cjce.5450760316.

Bellman R., Kashef B.G., Casti J, 1972. Differential quadrature: A technique for the rapid solution of nonlinear partial differential equations. *J. Comput. Phys*., 10, 40-52. DOI: 10.1016/0021-9991(72)90089-7.

Bourne J.R., 2003. Mixing and the selectivity of chemical reactions. *Org. Proc. Res. Dev.*, 7, 471-508. DOI: 10.1021/op020074q.

Cheng Q., Xu S., Shi J., Li W., Zhang J., 2013. Pump capacity and power consumption of two commercial in-line high shear mixers. *Ind. Eng. Chem. Res*., 52, 525–537. DOI: 10.1021/ie3023274.

Fournier M.C., Falk L., Villermaux J., 1996. A new parallel competing reaction system for assessing micromixing efficiency - Experimental approach. *Chem. Eng. Sci*., 51, 5053-5064. DOI: 10.1016/0009-2509(96)00270-9.

Jasińska M., Bałdyga J., Cooke M., Kowalski A., 2013a. Application of test reactions to study micromixing in the rotor-stator mixer (test reactions for rotor-stator mixer). *Appl. Therm. Eng*., 57, 172-179. DOI: 10.1016/j.applthermaleng.2012.06.036.

Jasińska M., Bałdyga J., Cooke M., Kowalski A., 2013b. Investigations of mass transfer with chemical reactions in two-phase liquid-liquid systems. *Chem. Eng. Res. Des*., 91, 2169- 2178. DOI: 10.1016/j.cherd.2013.05.010.

Jasińska M., Bałdyga J., Cooke M., Kowalski A., 2016. Mass transfer and chemical test reactions in the continuous-flow rotor-stator mixer. *Theor. Found. Chem. Eng.*, 50, 901-906. DOI: 10.1134/S0040579516060075.

Jasińska M., Bałdyga J., Hall S., Pacek A.W, 2014. Dispersion of oil droplets in rotor-stator mixers: Experimental investigations and modeling. *Chem. Eng. Process. Process Intensif.*, 84, 45-53. DOI: 10.1016/j.cep.2014.02.008.

Jasińska M., 2015. Test reactions to study efficiency of mixing. *Chem. Process Eng.*, 36, 171-208. DOI: 10.1515/cpe-2015-0013.

Kolmogorov A.N., 1949. Disintegration of drops in turbulent flows. *Dokl. Akad. Nauk SSSR*, 66, 825-828.

Ottino J.M., Macosko C.W, 1980. An efficiency for batch mixing of viscous fluids. *Chem. Eng. Sci*., 35, 1454-1457. DOI: 10.1016/0009-2509(80)85142-6.

Polyanin A.D., 1984. Three-dimensional diffusive boundary-layer problems. *Zhurnal Prikladnoi Mekhaniki i Tekhnicheskoi Fiziki*,4, 71-81.